Optimization and Engineering (2021) 22:2321–2347
https://doi.org/10.1007/s11081-021-09639-7

RESEARCH ARTICLE

The intensity-based measure approach to "Weberize" L^2-based methods of signal and image approximation

Dongchang Li[1] · Davide La Torre[2] · Edward R. Vrscay[1]

Received: 11 January 2021 / Revised: 7 April 2021 / Accepted: 23 April 2021 /
Published online: 3 May 2021

Abstract

We consider the problem of modifying L^2-based approximations so that they "conform" in a better way to Weber's model of perception: Given a greyscale background intensity $I > 0$, the minimum change in intensity ΔI perceived by the human visual system (HVS) is $\Delta I / I^a = C$, where $a > 0$ and $C > 0$ are constants. A "Weberized distance" between two image functions u and v should tolerate greater (lesser) differences over regions in which they assume higher (lower) intensity values in a manner consistent with the above formula. In this paper, we modify the usual integral formulas used to define L^2 distances between functions. The pointwise differences $|u(x) - v(x)|$ which comprise the L^2 (or L^p) integrands are replaced with measures of the appropriate greyscale intervals $\nu_a(\min\{u(x), v(x)\}, \max\{u(x), v(x)\}]$. These measures ν_a are defined in terms of density functions $\rho_a(y)$ which decrease at rates that conform with Weber's model of perception. The existence of such measures is proved in the paper. We also define the "best Weberized approximation" of a function in terms of these metrics and also prove the existence and uniqueness of such an approximation.

Keywords Weber model of perception · Range-dependent measures · Weberized image metrics · Best Weberized approximation · Abel's functional equation

✉ Edward R. Vrscay
ervrscay@uwaterloo.ca

Dongchang Li
d235li@uwaterloo.ca

Davide La Torre
davide.latorre@skema.edu

[1] Department of Applied Mathematics, Faculty of Mathematics, University of Waterloo, Waterloo, ON N2L 3G1, Canada

[2] SKEMA Business School, Université Côte d'Azur, Sophia Antipolis, France

1 Introduction

In this paper, we present a method of modifying, or "Weberizing," L^2-based approximations so that they conform as much as possible to Weber's model of perception. The term "Weberized" has been used in some recent papers which have incorporated Weber's model into classical image processing methods, namely, total variation (TV) restoration Shen (2003) and Mumford-Shah segmentation Shen and Jung (2006).

By Weber's model of perception we mean the following: Given a greyscale background intensity $I > 0$, the minimum change in intensity ΔI perceived by the human visual system (HVS) is related to I as follows,

$$\frac{\Delta I}{I^a} = C, \tag{1}$$

where $a > 0$ and C is constant, or at least roughly constant over a significant range of intensities I. The case $a = 1$ corresponds to the standard Weber model—often referred to as "Weber's law"—which is employed in practically all applications Wandell (1995). Even in this standard case however, different values of the constant C may hold over different regions of intensity space Li et al. (2014). There are also situations in which other values of a, in particular $a = 0.5$, may apply—see, for example, Michon (1966). These complications are beyond the scope of this paper which focuses on the model in Eq. (1).

Weber's law, $a = 1$ in Eq. (1), has been incorporated in a variety of imaging applications over the years. A couple of applications have already been mentioned Shen (2003); Shen and Jung (2006). The method of homomorphic filtering Oppenhein et al. (1968) incorporates the logarithmic transform of images, which is a special case of the generalized Weber metrics obtained from our approach, as will be shown below. The logarithmic image filter Pinoli (1997), motivated in part by the problem of how to perform various operations on images (including addition and subtraction) in accordance with perceptual characteristics of the HVS, is naturally consistent with Weber's law. In some situations, however, e.g., luminance and contrast discrimination Cornsweet and Pinsker (1965); Kingdom and Whittle (1996) and duration discrimination Halpern and Darwin (1982), the need to employ a-values different from 1, i.e., a departure from "Weber's law", has been recognized.

It is also well known that traditional L^2-based distance measures such as mean squared error (MSE) and peak signal-to-noise ratio (PSNR) perform poorly in terms of characterizing image quality (Girod 1993; Wang and Bovik 2009). The structural similarity (SSIM) measure Wang et al. (2004); Wang and Li (2011), which is acknowledged to demonstrate superior performance in comparison with these methods, has a "Weberized" component, namely, the luminance term, denoted as $S_1(\mathbf{x}, \mathbf{y})$, which characterizes the similarity between the mean values, $\bar{\mathbf{x}}$ and $\bar{\mathbf{y}}$, of image patches/blocks $\mathbf{x}$ and $\mathbf{y}$, respectively. The fact that $S_1(\mathbf{x}, \mathbf{y})$ may be expressed as a function of the ratio $\bar{\mathbf{x}}/\bar{\mathbf{y}}$ (or $\bar{\mathbf{y}}/\bar{\mathbf{x}}$) accounts for its Weberized form, with $a = 1$. Here

we mention that our Weberized approaches operate at the pixel level as opposed to mean values of blocks.

The basis of our entire program to Weberize metrics is as follows. Eq. (1) implies that the HVS will be less (more) sensitive to a given change in intensity ΔI in regions of an image at which the local image intensity $I(x)$ is higher (lower). As such, a Weberized distance between two functions u and v should tolerate greater/lesser differences over regions in which they assume higher/lower intensity values. The degree of toleration will be determined by the exponent a.

In this paper, we Weberize the L^2 metric by employing measures that are supported on the (positive) range space $\mathbb{R}_g = [A, B]$ of the functions to reformulate the integrals which normally define the L^2 distance between two functions. Some of the main ideas of range-based measures have appeared in Li et al. (2018) and Li et al. (2019) and have been discussed in much more detail in Li (2020). Here, we present some more mathematical details involved in the proof of existence of the range space measures. We also present the theoretical basis of the best approximation problem for Weberized measures and prove the existence and uniqueness of best Weberized approximations.

At this point, it is important to mention that another method has been devised to Weberize L^2-based metrics, namely, the use of intensity-dependent weight functions that are inserted into the distance integral. This method was first introduced in Kowalik-Urbaniak et al. (2014) for the standard Weber model, i.e., $a = 1$ in Eq. (1), and then analyzed in more detail in Kowalik-Urbaniak (2014). The extension of this weight function method to the generalized case $a > 0$ has recently been reported along with a proof of the existence and uniqueness of associated best Weberized approximations Urbaniak et al. (2020).

2 Mathematical preliminaries

The basic mathematical ingredients of our formalism are listed below.

1. The *base (or pixel) space* $X \subset \mathbb{R}^n$ on which our signals/images are supported. Here, without loss of generality since our discussion is purely theoretical, we simply consider the one-dimensional case $X = [0, 1] \subset \mathbb{R}$. The extension to higher-dimensional cases is rather straightforward. We also mention that our discussion easily extends to the discrete case encountered in practice, where X is comprised of pixels or voxels—for example, $X = \{1, 2, \ldots, n_1\} \times \{1, 2, \ldots, n_2\}$, in which case the images are $n_1 \times n_2$ arrays of numbers.
2. The *(greyscale or intensity) range space* For an $A > 0$, $\mathbb{R}_g = [A, B]$, where $B < \infty$. Once again, our discussion can be extended to the discrete case, e.g., N bit-per-pixel digital images for which $\mathbb{R}_g = \{0, 1, \ldots, 2^N - 1\}$.
3. *Set of (signal/image) functions* $\mathcal{F}(X) = \{u : X \to \mathbb{R}_g \mid u \text{ measurable }\}$. From our definition of the greyscale range $\mathbb{R}_g$, $u \in \mathcal{F}(X)$ is positive and bounded almost everywhere, i.e., $0 < A \leq u(x) \leq B < \infty$ for almost every $x \in X$. A consequence

of this boundedness is that $\mathcal{F}(X) \subset L^p(X)$ for all $p \geq 1$, where the $L^p(X)$ function spaces are defined in the usual way. In this paper, we shall be using the L^2 metric,

$$d_2(u,v) = \|u - v\|_2 = \left[\int_X [u(x) - v(x)]^2 \, dx\right]^{1/2}, \quad u, v \in \mathcal{F}(X). \tag{2}$$

It is important to mention that because of the restrictions on the range values, $\mathcal{F}(X)$ is not a linear space: For $u, v \in \mathcal{F}(X)$, it does not follow that $c_1 u + c_2 v \in \mathcal{F}(X)$ for all $c_1, c_2 \in \mathbb{R}$. Moreover, the zero function is not an element of $\mathcal{F}(X)$. As will be seen below, the restriction to nonnegative range values is necessary because of the form of the weight functions used in our Weberized distance integrals.

The following result, which establishes some additional properties of the space $\mathcal{F}(X)$ in which we are working, is proved in Li (2020).

Theorem 1 *The set $\mathcal{F}(X)$ is bounded, closed and convex.*

3 Metrics on $\mathcal{F}(X)$ defined in terms of intensity-based measures

In this paper, we consider a range-dependent (or greyscale-dependent, intensity-dependent) metric on the space $\mathcal{F}(X)$ to be described below. The idea for this metric comes from Forte and Vrscay (1995), in which the authors considered metrics on function spaces involving level sets.

Consider two functions $u, v \in \mathcal{F}(X)$ and define the following subsets of the base space $X = [a, b]$:

$$X_u = \{x \in X \mid u(x) \leq v(x)\} \qquad X_v = \{x \in X \mid v(x) \leq u(x)\}, \tag{3}$$

so that $X = X_u \cup X_v$. A generic situation is sketched in Fig. 1.

The distance D between u and v will be defined as an integration over vertical strips of width dx and centered at $x \in [a, b]$. The contribution of each strip will **not**, in general, be determined by the usual lengths of the strips, i.e., the quantities $|u(x) - v(x)|$, but rather the **sizes** of the intervals $(u(x), v(x)] \subset \mathbb{R}_g$ and $(v(x), u(x)] \subset \mathbb{R}_g$ as assigned by a non-atomic **measure** ν that is supported on the

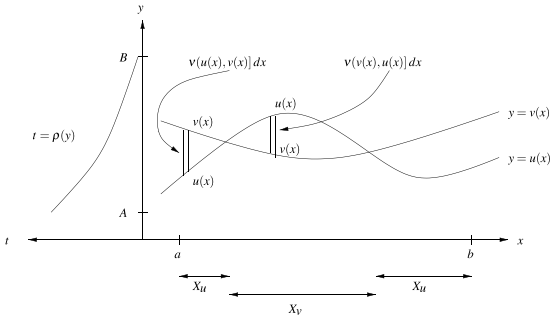

Fig. 1 Sketch of two functions $u(x), v(x) \in \mathcal{F}(X)$ with strips of width dx that will contribute to the distance $D(u, v; \nu)$. A density function $\rho(y)$ over the greyscale range $\mathbb{R}_g = [A, B]$ is sketched at the left

range interval $\mathbb{R}_g = [A, B]$. We shall refer to ν as the **intensity-based measure** on $\mathbb{R}_g$. The measures of the two intervals shown in the figure will be denoted as $\nu(u(x), v(x)]$ and $\nu(v(x), u(x)]$, respectively. The distance between u and v associated with the measure ν is now defined as follows,

$$D(u, v;\nu) = \int_{X_u} \nu(u(x), v(x)]\, dx \; + \; \int_{X_v} \nu(v(x), u(x)]\, dx\,. \tag{4}$$

Theorem 2 *Let $\nu \in \mathcal{B}(\mathbb{R}_g)$, the set of Borel measures on $\mathbb{R}_g$ such that ν is nonatomic on $\mathbb{R}_g$. Then $D(u, v;\nu)$ defined in* Eq. (4) *is a metric on $\mathcal{F}(X)$.*

Proof The only nontrivial property to show is the triangle inequality. To show this, consider the cumulative distribution function (CDF) associated with ν on $\mathbb{R}_g$:

$$F(y) = \int_0^y d\nu\,, \quad y \in \mathbb{R}_g = [A, B]\,, \tag{5}$$

so that $F(a) = 0$ and $F(b) = 1$. Since ν is assumed to be nonatomic, $F(y)$ is a continuous and nondecreasing function on $\mathbb{R}_g$. Then from Eq. (4), and for any $u, v, w \in \mathcal{F}(X)$,

$$\begin{aligned} D(u, v;\nu) &= \int_X |F(u(x)) - F(v(x))|\, d\nu \\ &= \int_X |F(u(x)) - F(w(x)) + F(w(x)) + F(v(x))|\, d\nu \\ &\le \int_X |F(u(x)) - F(w(x))|\, d\nu + \int_X |F(w(x)) - F(v(x))|\, d\nu \\ &= D(u, w;\nu) + D(w, v;\nu)\,. \end{aligned} \tag{6}$$

The proof is complete. □

In the applications considered in this paper, we shall be employing measures which are defined by continuous, non-negative density functions $\rho(y)$ for $y > 0$. Given a measure ν with associated density function ρ, then for any interval $(y_1, y_2] \subset \mathbb{R}_g$,

$$\nu\,(y_1, y_2] = \int_{y_1}^{y_2} \rho(y)\, dy \; = P(y_2) - P(y_1)\,, \tag{7}$$

where $P'(y) = \rho(y)$. The metric $D(u, v;\nu)$ in Eq. (4) then becomes

$$D(u, v;\nu) = \int_X |P(u(x)) - P(v(x))|\, dx\,. \tag{8}$$

Special Case $\nu = m_g$, uniform Lebesgue measure on $\mathbb{R}_g$. Here, $\rho(y) = 1$ so that $P(y) = y$ in Eq. (8). This is the measure on $\mathbb{R}_g$ employed in most, if not almost all, function metrics, e.g., the standard L^p metrics. The associated metric is

$$D(u, v, m_g) = \int_X |u(x) - v(x)|\, dx = \|u - v\|_1 , \tag{9}$$

the L^1 distance between u and v.

The following L^p-type generalizations of the metric D in Eq. (8) may be defined in terms of the CDF of the measure ν: For $p \geq 1$, and $u, v \in \mathcal{F}(X)$,

$$D_p(u, v; \nu) = \left[\int_X |P(u(x)) - P(v(x))|^p \, d\nu \right]^{1/p} . \tag{10}$$

That D_p is a metric on $\mathcal{F}(X)$ for $p \geq 1$ can easily be shown by using the method employed in the Proof of Theorem 2. Later in this paper, we shall be particularly interested in the case $p = 2$.

4 Measures/density functions which accommodate Weber's models of perception

As discussed in Li et al. (2018), the constancy of the Lebesgue density function $\rho(y) = 1$ implies that all greyscale intensity values are weighted equally in the computation of distances between image functions. However, Weber's model of perception in Eq. (1) suggests that for $a > 0$, the density function $\rho_a(y)$ defining the intensity-based measure ν_a should be a **decreasing** function of intensity y: As the intensity value increases, the HVS will tolerate greater differences between $u(x)$ and $v(x)$ before being perceived. How the density function $\rho_a(y)$ will capture this decrease in perception is based on the following observation Kowalik-Urbaniak et al. (2014).

Special case $a = 1$: Let ν be the measure on $\mathbb{R}_g$ with density function $\rho(y) = 1/y$. Let $I \in \mathbb{R}_g$. From Weber's standard law, $a = 1$ in Eq. (1), the minimum change in perceived intensity at I is $\Delta I = CI$. Note that

$$\nu([I, I + \Delta I]) = \int_I^{I+\Delta I} \frac{1}{y}\, dy = \int_I^{I+CI} \frac{1}{y}\, dy = \ln(1 + C) , \tag{11}$$

which is independent of I. (We have assumed that $I + \Delta I \in \mathbb{R}_g$.) This **perceptual invariance result** may be viewed graphically in terms of an "equal area" condition over $\mathbb{R}_g$ involving the density function $\rho(y)$. To see this, let $I_1, I_2 \in \mathbb{R}_g$. From Weber's standard law, $a = 1$ in Eq. (1), the minimum changes in perceived intensity at I_1 and I_2 are $\Delta I_1 = CI_1$ and $\Delta I_2 = CI_2$, respectively, so that

$$\int_{I_1}^{I_1+\Delta I_1} \frac{1}{y} dy = \int_{I_2}^{I_2+\Delta I_2} \frac{1}{y} dy = \ln(1 + C) . \tag{12}$$

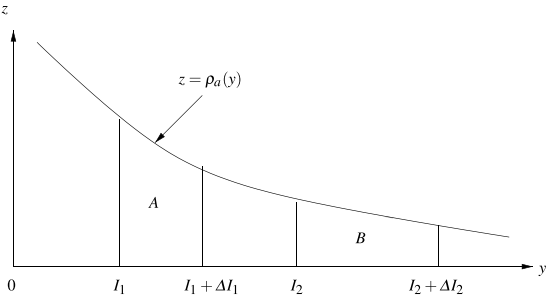

Fig. 2 Graphical interpretation of the "equal area" invariance result in Eq. (12). Area of A = Area of B

In Fig. 2 below, the areas of the regions lying above the intervals $[I_1, I_1 + \Delta I_1]$ and $[I_2, I_2 + \Delta I_2]$ and below the graph of the density function $\rho(y)$ are equal.

For the case $a = 1$, the density function $\rho(y) = 1/y$ decreases in an "appropriate manner" in order to produce this equal area situation. We say that the measure ν, or its density function $\rho(y) = 1/y$, **conforms to** or **accommodates** Weber's standard law in the case $a = 1$. The metric D in Eq. (8) defined by this measure is

$$D(u, v, \nu) = \int_X |\ln u(x) - \ln v(x)|\, dx\,. \tag{13}$$

These observations lead us to propose the following "equal area" definition for Weber's generalized model of perception, i.e., $a \neq 1$.

Definition For a given $a > 0$, suppose that Weber's model of perception in Eq. (1) holds for a particular value of $C > 0$ for all values of $I \geq A$. (See Note 3 below.) We say that a measure $\nu_a(y)$ defined by the density function $\rho_a(y)$ **conforms to** or **accommodates** this Weber model if the following condition holds for all $I \geq A$,

$$\nu_a(I, I + \Delta I) = \int_I^{I+\Delta I} \rho_a(y)\, dy = K\,, \tag{14}$$

for some constant K, where $\Delta I = CI^a$ is the minimum change in perceived intensity at I according to Eq. (1).

We view Eq. (14) as a **generalized perceptual invariance property** of intensity-based measures which conform to Weber's model. Once again, it admits a graphical interpretation in terms of equal areas enclosed by the density curve $\rho_a(y)$ as shown in Fig. 2.

Notes

1. As shown earlier, in the special case, $a = 1$, i.e., Weber's standard model, $\rho_1(y) = 1/y$ and $\nu(I, I + \Delta I) = \ln(1 + C)$ Li et al. (2018).

2. We may also include the special case $a = 0$, i.e., an absence of Weber's model, in the above definition. In this case $\rho_0(y) = 1$ so that $\nu = m_g$, Lebesgue measure on $\mathbb{R}_g$. Here, $\Delta I = CI^0 = C$ so that $\nu(I, I + \Delta I) = \nu(I, I + C) = C$.
3. As mentioned earlier, Weber's model in Eq. (1) is valid only over a limited range of intensities. The requirement that Eq. (14) be true for all $I > A$ is imposed to help establish the asymptotic behaviour of the density functions $\rho_a(y)$ for large y.

From Notes 1 and 2 above, it is natural to conjecture that for $a > 0$ in general, $\rho_a(y) = 1/y^a$ or at least approaches $1/y^a$ asymptotically as $y \to \infty$. It is easy to show that equality does not hold for $a \neq 1$. Nevertheless, the conjectured asymptotic behaviour does hold in the case $0 < a < 1$ as we discuss in Sect. 4.2 below.

The following result, although seemingly trivial, will have some important consequences. It is proved in Li (2020).

Theorem 3 *For given values of $a > 0$ and $C > 0$, let $\rho_a(y)$ satisfy the invariance condition in* Eq. (14). *Then* $\int_A^\infty \rho_a(y)\, dy = \infty$.

Proof A sketch of the proof is as follows. Let $y_0 = A$, and $y_{n+1} = y_n + Cy_n^a$ for $n \geq 0$. It is not difficult to show that $y_n \to \infty$ as $n \to \infty$. Furthermore, from Eq. (14),

$$\int_A^{y_n} \rho_a(y)\, dy = nK \to \infty \quad \text{as} \quad n \to \infty\,, \tag{15}$$

which completes the proof. □

This result establishes that the asymptotic property $\rho_a(y) \sim 1/y^a$ as $y \to \infty$ cannot hold for $a > 1$.

In preparation for the main result of this section of the paper, let $g(y)$ be a continuous function on $[A, \infty)$ and consider its particular antiderivative defined as follows,

$$G(x) = \int_A^x g(y)\, dy \quad x \geq A > 0\,. \tag{16}$$

Clearly, $G(A) = 0$. Furthermore, suppose that for fixed values of $a > 0$ and $C > 0$, $g(y)$ satisfies the invariance property in Eq. (14). It follows that $G(x)$ satisfies the following equation,

$$G(x + Cx^a) - G(x) = K\,, \quad x \geq A\,. \tag{17}$$

For convenience, we define

$$f(x) = x + Cx^a \tag{18}$$

and divide both sides of Eq. (17) by K to obtain the equation,

$$H(f(x)) - H(x) = 1\,, \tag{19}$$

where $H(x) = K^{-1}G(x)$. Eq. (19) is known as **Abel's equation**, a well known functional equation Targonski (1981).

Abel's equation in (19) is said to be **solvable** if, given the function $f(x)$, a continuous solution $H(x)$ satisfies it for all $x \in X \subset \mathbb{R}$. Note that if $H(x)$ is a solution to (19), then so is $H(x) + C$, where $C \in \mathbb{R}$ is a constant.

Very briefly, the existence of a continuous solution to Abel's equation depends on some properties of the function $f(x)$, in particular its **iteration dynamics**. To see this, let us rewrite Eq. (19) as

$$H(f(x)) = H(x) + 1 \tag{20}$$

and then replace x with $f(x)$—assuming that $f(x) \in X$—to obtain

$$H(f^2(x)) = H(f(x)) + 1 = H(x) + 2\,, \tag{21}$$

where $f^2(x) = f(f(x))$. Repeating this procedure n times – again assuming that the iterates $f^k(x)$ lie in X—yields

$$H(f^n(x)) = H(x) + n\,, \quad n \geq 1\,. \tag{22}$$

It follows that for a continuous solution to (19) to exist, the function f cannot have a periodic point, i.e., a point p such that there exists an $n \geq 1$ for which $f^n(p) = p$. (A fixed point $f(p) = p$ is a particular example of a periodic point.) For if such a periodic point exists then from Eq. (22),

$$H(p) = H(p) + n\,, \quad n \geq 1\,, \tag{23}$$

which has no solution, implying that $H(p)$ is undefined.

Another important point is that the space X cannot be compact. For example, suppose that X is the interval $[a, b]$. Then for an $x_0 \in X$, all iterates $f^n(x_0) \in X$, $n \geq 0$. There must exist a subsequence $x_{n_k} = f^{n_k}(x_0)$, $k \geq 0$, which converges to a limit point $\bar{x} \in X$. Assuming that f is continuous, $f(\bar{x}) = \bar{x}$, i.e., $\bar{x}$ is a fixed point of f. From the discussion in the previous paragraph, it follows that $H(\bar{x})$ is undefined. (This is why the equal-area condition in Eq. (14) is formulated over $[A, \infty)$ and not $[A, B]$.)

In our case, the dynamics of iteration of the function $f(x)$ in Eq. (18)—which arises from the generalized Weber's model of perception—is such that solutions to Abel's equation in (19) are guaranteed. This will be discussed in more detail in the proof of Theorem 5 below. From the relationship between $H(x)$ and $G(x)$ in Eq. (16), this implies the existence of a density function $g(x)$ which satisfies the equal area condition of Eq. (14). Our analysis of Eq. (19), however, provides no insight into the nature of this density function. For example, is it continuous? Is it unique?

In order to answer these questions, we consider the following linear functional equation in $g(x)$ for $x \geq A$,

$$g(x + Cx^a)(1 + aCx^{a-1}) - g(x) = 0\,. \tag{24}$$

Although this equation may be obtained by formally differentiating both sides of Eq. (17), we consider Eq. (17) to be obtained by formally antidifferentiating both sides of Eq. (24).

Equation (24) is a special case of the following family of linear functional equations studied by Belitskii and Lyubich in Belitskii and Lyubich (1988),

$$P(x)\psi(f(x)) + Q(x)\psi(x) = \gamma(x)\,, \quad x \in X\,, \tag{25}$$

where X is the topological space over which the equation is being considered. In our case, $X = [A, \infty)$, $f(x) = x + Cx^a$ (cf. Eq. 18), $P(x) = f'(x) = 1 + aCx^{a-1}$, $Q(x) = -1$ and $\gamma(x) = 0$. In Belitskii and Lyubich (1988), it is shown that if the Abel equation associated with Eq. (25), namely,

$$\phi(f(x)) - \phi(x) = 1\,, \quad x \in X\,, \tag{26}$$

has a continuous solution $\phi(x)$, then Eq. (25) is said to be totally solvable, i.e., it has a continuous solution $\psi(x)$ for every continuous function $\gamma(x)$. Note that Eq. (26) is identical to Eq. (19) examined earlier.

The following definitions are required for the Theorem which follows.

Definition 1 A metric space X is said to be countable at infinity if there exists a covering,

$$X = \bigcup_{i=1}^{\infty} K_i\,, \tag{27}$$

where the K_i are compact.

Definition 2 Let X be a metric space and $f : X \to X$. A compact set $U \subset X$ is said to be wandering (under the action of f) if there exists a number $N > 0$ such that

$$f^n(K) \bigcap f^m(K) = \emptyset \quad \text{(null set)} \tag{28}$$

for all $n, m \in \mathbb{N}$ such that $|n - m| \geq N$. Here f^n denotes the n-fold composition of f with itself.

The following Theorem, which is presented as Corollary 1.6 in Belitskii and Lyubich (1988), will establish the solvability of Eq. (26) and total solvability of Eq. (25).

Theorem 4 *Assume that the space X is locally compact and countable at infinity and that $f : X \to X$ is injective. Then the following statements are equivalent*:

1. *Any nondegenerate* Eq. (25) *is totally solvable*.
2. *Abel's* Eq. (26) *is solvable*.
3. *Under the action of f, every compact set in X is wandering*.

We now use the above result to derive the main results of this section of the paper.

Theorem 5 *Let* $X = [A, \infty)$, $a > 0$ *and* $C > 0$. *Then for* $f(x) = x + Cx^a$, $P(x) = 1 + aCx^{a-1}$ *and* $Q(x) = -1$, *the functional equation in* (25) *is totally solvable, implying that a continuous solution exists for the special case* $\gamma = 0$, *namely* Eq. (24).

Proof First of all, the space $X = [A, \infty) \subset \mathbb{R}$ is locally compact and countable at infinity. (For example, let $K_i = [iA, (i+1)A]$ for $i \geq 1$.) Secondly, $f(x) = x + Cx^a > x$ for all $x > 0$ which implies that $f : X \to X$. More precisely, $f : [A, \infty) \to [f(A), \infty)$. Thirdly, $f'(x) = 1 + aCx^{a-1} > 0$ for all $x > 0$ which implies that $f(x)$ is strictly increasing for all $x > 0$. Therefore f is injective. From these properties, Theorem 4 is applicable to our problem. We now show that Statement No. 3 holds for the mapping $f : X \to X$.

Since $f(x) > x$ for all $x \in X$, it follows that the iteration sequence defined by $x_{n+1} = f(x_n)$ is strictly increasing. (Consequently f cannot have any periodic points in X.) Moreover, since $x_{n+1} - x_n = Cx_n^a$, it follows that $x_n \to \infty$ as $n \to \infty$. Finally, note that $f'(x) > 0$ for $x > 0$ which implies that $f(x)$ is increasing on $X = [A, \infty)$.

Define the intervals $I_n = [f^n(A), f^{n+1}(A)]$ for $n \geq 0$. It follows that $f : I_n \to I_{n+1}$ for $n \geq 0$—a kind of "Bernoulli right-shifting" of the intervals.

Now let $K \subset X$ be compact. Let $L \geq 0$ and $M > L$ be, respectively, the largest and smallest integers so that $K \subset \cup_{n=L}^{M} I_n$ and $K \cap f^{M+1}(A) = \emptyset$. From this construction, $K \cap f^{M-L}(K) = \emptyset$ from which it follows that $f^n(K) \cap f^m(K) = \emptyset$ for all n, m such that $|n - m| \geq M - L > 1$. Therefore K is wandering. Since K is arbitrary, Statement No. 3 in Theorem 4 is satisfied. Therefore Abel's equation (26) is solvable and the functional equation in (25) is totally solvable. □

Theorem 6 *For given values of* $a > 0$ *and* $C > 0$, *there exists a continuous function* $\rho_a(y)$ *defined on* $[A, \infty)$ *which satisfies* Eq. (14).

Proof From Theorem 5, there exists a continuous function g which satisfies Eq. (24) and which we shall rewrite as follows,

$$g(f(x))f'(x) = g(x), \quad x \geq A, \tag{29}$$

where, as before, $f(x) = x + Cx^a$. For any $I \geq A$, integrate both sides of Eq. (29) from $x = A$ to $x = I$ to produce the following result,

$$\int_{f(A)}^{f(I)} g(x)\,dx = \int_{A}^{I} g(x)\,dx. \tag{30}$$

Now rewrite the LHS of the above equation as follows,

$$\int_{f(A)}^{I} g(x)\,dx + \int_{I}^{f(I)} g(x)\,dx = \int_{A}^{I} g(x)\,dx. \tag{31}$$

Subtracting the first definite integral from both sides of the equation yields

$$\int_I^{f(I)} g(x)\,dx = \int_A^{f(A)} g(x)\,dx = K \quad \text{constant}\ , \tag{32}$$

for any $I \geq A$. This is precisely the equal area condition of Eq. (14) with $\Delta I = CI^a$. Therefore, the Weber density function $\rho_a(y)$ in Eq. (14) is given by the solution $g(y)$ to Eq. (24). □

4.1 Some comments on Theorem 6 and the nonuniqueness of Weberized density functions

The reader will note that in Theorems 5 and 6 there is no mention of uniqueness of solutions. Indeed, if $g(x)$ is a solution to Eq. (29) then $cg(x)$ is also a solution, where $c \in \mathbb{R}$ is an arbitrary constant. $g(x) = 0$ is the trivial solution. These are consequences of the fact that Eq. (24), the original form of Eq. (29), is a linear, homogeneous functional equation in g. Different nonzero values of c will result in different values of the constant K in Eq. (14).

In light of the above point one might hope, in the usual desire to establish uniqueness, that the solution to Eq. (29) be unique, at least up to a multiplicative constant. Unlike the situation for differential equations, however, linear, homogeneous functional equations can admit an infinity of "different," i.e., linearly independent, solutions. As mentioned earlier, it is the function $f(x)$ which determines the existence and uniqueness of solutions. In our case, where $f(x) = x + Cx^a$ with $a > 0$ and $C > 0$ fixed, an infinity of linearly independent solutions actually exists. We now discuss this matter a little further.

Given a solution $g(x)$, let us assume the existence of a second solution $h(x) = g(x)u(x)$, where $u(x)$ is to be determined. Substitution into (29) yields

$$g(f(x))u(f(x))f'(x) = g(x)u(x)\,, \quad x \geq A\,. \tag{33}$$

From Eq. (29), it follows that

$$u(f(x)) = u(x)\,, \quad x \geq A\,. \tag{34}$$

This is the homogeneous functional equation corresponding to Abel's equation in (26). We now employ a method similar to the one outlined in Section 3.3 of Small (2007) (top of Page 61) to show that an infinite number of solutions of Eq. (34) can be constructed.

As in the Proof of Theorem 5, define the intervals $I_n = [f^n(A), f^{n+1}(A)]$ for $n \geq 0$, where $f(x) = x + Cx^a$ for $x \geq A$. Recall that $f : I_n \to I_{n+1}$ for $n \geq 0$. Furthermore f is bijective. Now let $u(x)$ be defined as follows for $x \geq A$:

1. Let $q(x)$ be **any** continuous function on $I_0 = [A, f(A)]$ such that $q(A) = q(f(A))$. From the continuity of q and the compactness of I_0, there exists an $M > 0$ such that $|q(x)| \leq M$ for all $x \in I_0$. Define $u(x) = q(x)$ for $x \in I_0$.
2. We now iterate the following procedure for $n = 1, 2, 3, \ldots$: Let $u(x)$ be defined on I_n as follows,

$$u(x) = u(f^{-1}(x)), \quad \forall x \in I_n\,. \tag{35}$$

In other words, the values of $u(x)$ on I_n are obtained from the values of $u(x)$ on I_{n-1}. It follows that $|u(x)| \le M$ for all $x \ge A$.

By construction, u satisfies Eq. (34) for all $x \ge A$: Simply replace x with $f(x)$ in Eq. (35) to see this. Furthermore, u is continuous at all $x > A$. Therefore $h(x) = u(x)g(x)$ is a continuous function on $[A, \infty)$ which satisfies Eq. (29).

Finally, if g_1 and g_2 are solutions of Eqs. (29) or (24), then for any pair $c_1, c_2 \in \mathbb{R}$ (or $\mathbb{C}$), the linear combination $c_1 g_1 + c_2 g_2$ is also a solution. In other words, the solutions to this linear, homogeneous functional equation form a vector space (which is reminiscent of differential equations). Because of the flexibility in the choice of u, this vector space has infinite dimensionality.

In closing this section, we remark that the nonuniqueness of solutions is not a problem since our asymptotic method, outlined in the next section, produces a family of positive, monotonically decreasing solutions that are perfectly suited for our applications.

4.2 Asymptotic behaviour of Weber density functions $\rho_a(y)$

We first remind the reader that only in the cases $a = 0$ and $a = 1$ is $\rho_a(y)$ is known exactly: Up to multiplicative factors, $\rho_0(y) = 1$ and $\rho_1(y) = 1/y$. For all other a-values, we must resort to asymptotic analysis to determine at least the leading behaviour of the density functions. The determination of the asymptotic behaviour of $\rho_a(y)$ is centered on the equal area property in Eq. (14). Here we summarize our work and its results.

In our first efforts, as reported in Li et al. (2018), we employed a "reverse technique" by assuming that $\rho_a(y) = 1/y^a$ in Eq. (14) and determining the asymptotic behaviour of $\Delta I = Cf(I)$ as $I \to \infty$ such that Eq. (14) be satisfied for all $I \ge A > 0$. Differentiation with respect to I yields a differential equation for $f(I)$. For $0 < a < 1$, $f(I) \sim I^a$ as $I \to \infty$, in accordance with Weber's model in Eq. (1), thus yielding the following result.

Theorem 7 *For* $0 < a < 1$, *the density function* $\rho_a(y)$ *which accommodates Weber's model of perception according to* Eq. (14) *is, to leading order,* $\rho_a \sim 1/y^a$ *as* $y \to \infty$.

This result is actually sufficient for the construction of our Weberized metrics since, as we discuss in Section 5, only the leading-order terms of the density function $\rho_a(y)$ are used. Nevertheless, later work was devoted to the determination of more terms in the asymptotic expansion of $\rho_a(y)$ using the integral in Eq. (14). The asymptotic results in the next section were presented in Li et al. (2019) along with a few details on how they were derived. A complete analysis is presented in Li (2020).

Finally, the functional equation approach described in the previous section was motivated by the desire to go one step further and establish a mathematical proof for the existence of density functions $\rho_a(y)$.

4.2.1 Asymptotic behaviour as $y \to \infty$

Case 1 For a given $a \in (0, 1)$ and $C > 0$, the asymptotic expansion of the Weber density function $\rho_a(y)$ satisfying Eq. (14) has the form,

$$\rho_a(y) = \sum_{n=0}^{\infty} \frac{A_n}{y^{a+n(1-a)}} \quad \text{as} \quad y \to \infty\,. \tag{36}$$

The first three terms of this expansion are

$$\rho_a(y) = \frac{1}{y^a} + \frac{1}{2}aC\frac{1}{y} - \frac{1}{12}aC^2(2a-1)\frac{1}{y^{2-a}} + \cdots\,. \tag{37}$$

Case 2 In the case $a > 1$, it follows from Theorem 3 that the leading behaviour of $\rho_a(y)$ cannot be of the form $1/y^a$. This case is difficult, and only the first two terms of the asymptotic expansion are known. For a given $a > 1$ and $C > 0$,

$$\rho_a(y) \simeq \frac{1}{y\,\ln y} - \left(\frac{\ln C}{a}\right)\frac{1}{y\,(\ln y)^2} \quad \text{as} \quad y \to \infty\,. \tag{38}$$

This result is interesting in that the leading-order term is independent of a, unlike the situation for $a \in [0, 1]$.

4.2.2 Asymptotic behaviour as $y \to 0^+$

There is a reciprocity with regard to the integrals involved in the previous analysis of $y \to \infty$ and those involved in the case $y \to 0^+$. It is quite straightforward to show, for example, that an analysis of the asymptotic limit $x \to 0^+$ for the case $0 < a < 1$ employs the same equations as those used in the analysis of $x \to \infty$ for the case $a > 1$. For this reason, we simply state the two major results below:

$$0 < a < 1: \quad \rho_a(y) \simeq -\frac{1}{y\,\ln y} - \left(\frac{\ln C}{a}\right)\frac{1}{y\,(\ln y)^2} \quad \text{as} \quad y \to 0^+\,,$$

$$a > 1: \quad \rho_a(y) = \frac{1}{y^a} + \frac{1}{2}aC\frac{1}{y} - \frac{1}{12}aC^2(2a-1)\frac{1}{y^{2-a}} + \cdots \text{ as } \quad y \to 0^+\,,$$

where the second result is the truncation of an asymptotic expansion having the same form as in Eq. (36), with the same coefficients A_n.

4.3 Some comments on these asymptotic results

The asymptotic analysis of the density functions $\rho_a(y)$ in the case $y \to 0^+$ is more of a theoretical exercise since we are working with the range space $\mathbb{R}_g = [A, B]$ with lower cutoff intensity level $A > 0$. Indeed, the validity of Weber's model for low intensity values is also questionable. We are more interested in the high-intensity region and expect that the behaviour of $\rho_a(y)$ is well described by the asymptotic formulas for $y \to \infty$. In fact, as was done in Li et al. (2018), we consider only the leading-order behaviour of the asymptotic expansions: Although it would be an interesting mathematical exercise, the inclusion of subdominant terms would most probably be "overkill" in practice, especially in light of the fact that Weber's model is, in itself, an approximation.

At this point, the reader may be wondering how these asymptotic results can be reconciled with our earlier comments on Theorem 6 as well as the discussion in Sect. 4.1 regarding the nonuniqueness of solutions to the functional equation in (24), hence density functions satisfying the "equal area condition" in Eq. (14). For $a > 0$, our asymptotic method produces a density function $\rho_a(y)$ which is continuous and decreasing and which satisfies Eq. (24) since it satisfies Eq. (17). As mentioned earlier, any constant multiple of this density function also satisfies the equal area condition in Eq. (14) for a different value of the constant K. Up to a multiplicative constant, the asymptotic expansions presented in Sects. 4.2.1 and 4.2.2 are unchanged. This one-parameter family of density functions is perfectly suited and sufficient for the construction our Weberized metrics in Section 5.

As discussed in Sect. 4.1, other (continuous) solutions to the functional equation in (24) may be produced by multiplying the $\rho_a(y)$ density functions by a continuous and nonconstant function $u(y)$ which is the solution to Abel's homogeneous equation in (34). From the construction of $u(y)$ for $y \geq A$ in Sect. 4.1, it follows that $u(y)$ is bounded for all $y \geq A$, i.e., there exists an $M \geq 0$ such that $|u(y)| \leq M$ for all $y \geq A$. It then follows that the density function $u(y)\rho_a(y)$ will, up to a multiplicative constant, also behave asymptotically according to the formulas of Sects. 4.2.1 and 4.2.2.

5 Generalized Weber metrics and the best approximation problem

We now consider the problem of finding best approximations—to be defined below—to a given "reference" or "target" function $u \in \mathcal{F}(X)$ with respect to the metrics defined by measures ν which conform to Weber's model of perception. We shall refer to such metrics as "generalized Weber metrics". These metrics will have the form of the D_p metrics in Eq. (10). At this point, we make three important choices:

1. Because of its special differentiability properties, we shall be using the $p = 2$ metric in Eq. (10).

2. For simplicity, we use only the **leading-order** term of the asymptotic expansion for the Weber-conforming density function $\rho_a(y)$ in the case $0 \le a \le 1$, i.e., we define

$$\rho_a(y) = \frac{1}{y^a} \quad \text{for} \quad 0 \le a \le 1\,. \tag{39}$$

3. In what follows, we consider only the cases $0 \le a \le 1$. For $a > 1$, the dominant asymptotic behaviour of $\rho_a(y)$ is $1/(y \ln y)$ which is independent of a. We can, in principle, work with this density function—it would imply that we work with the modified target function $\ln(\ln u(x))$. There is, however, no evidence that Weber's model is valid for $a > 1$.

With these comments in mind, our L^2-type generalized Weber metrics will have the following forms,

$$\begin{aligned} 0 \le a < 1: \quad D_{2,a}(u,v) &= \left[\int_X \left[u(x)^{-a+1} - v(x)^{-a+1}\right]^2 dx\right]^{1/2} \\ &= \|u^{a+1} - v^{a+1}\|_2 \\ a = 1: \quad D_{2,1}(u,v) &= \left[\int_X [\ln u(x) - \ln v(x)]^2\, dx\right]^{1/2} \\ &= \|\ln u - \ln v\|_2\,. \end{aligned} \tag{40}$$

The following results, which establish the equivalence of these metrics with the L^2 metric, were derived in Li et al. (2019) as consequences of the Mean Value Theorem.

Theorem 8 *For* $\mathbb{R}_g = [A, B]$, $0 < A < B < \infty$, *and* $0 < a \le 1$, *the metrics* $D_{2,a}$ *defined in* Eq. (40) *are equivalent to the usual* d_2 *metric on* $X \subset \mathbb{R}$. *More precisely, for* $u, v \in \mathcal{F}(X)$,

1. *For* $0 < a < 1$: $\dfrac{1-a}{B^a} d_2(u,v) \le D_{2,a}(u,v) \le \dfrac{1-a}{A^a} d_2(u,v)$.
2. *For* $a = 1$: $\dfrac{1}{B} d_2(u,v) \le D_{2,1}(u,v) \le \dfrac{1}{A} d_2(u,v)$.

We now show that the metrics $D_{2,a}$ also conform to Weber's model of perception in another manner, namely the one exhibited by the Weberized distance functions Δ_a in Urbaniak et al. (2020) which were constructed using intensity-dependent weight functions. Consider the "flat" reference image $u(x) = I$, where $I \in \mathbb{R}_g$. For an $a \in (0, 1]$, let $v(x) = I + \Delta I$ be the constant approximation to $u(x)$, where $\Delta I = CI^a$ is the minimum perceived change in intensity corresponding to Weber's model in Eq. (1). The L^2 distance between u and v is

$$d_2(u,v) = K \cdot \Delta I = KCI^a\,, \quad \text{where} \quad K = \left[\int_X dx\right]^{1/2}. \tag{41}$$

We now compute the generalized Weber distances between u and v.

1. *Case 1* $0 < a < 1$. Then

$$\begin{aligned} D_{2,a}(u,v) &= \left[\int_X [I^{-a+1} - (I+\Delta I)^{-a+1}]^2\, dx\right]^{1/2} \\ &= I^{-a+1}\left[\int_X \left[1 - \left(1 + \frac{CI^a}{I}\right)^{-a+1}\right]^2 dx\right]^{1/2} \\ &\sim I^{-a+1}\left[\int_X \left[(1-a)CI^{a-1}\right]^2 dx\right]^{1/2} \quad \text{as} \quad I \to \infty \\ &= (1-a)KC \quad \text{as} \quad I \to \infty\,, \end{aligned} \tag{42}$$

where K is given in Eq. (41). The third line in the derivation was obtained by using the following result from Taylor's theorem,

$$f(x) = (1+x)^\alpha = 1 + \alpha x + O(x^2) \quad \text{as} \quad x \to 0^+\,. \tag{43}$$

2. *Case 2* $a = 1$. Then

$$\begin{aligned} D_{2,1}(u,v) &= \left[\int_X [\ln I - \ln(I+\Delta I)]^2\, dx\right]^{1/2} \\ &= \left[\int_X [\ln I - \ln(I+CI)]^2\, dx\right]^{1/2} \\ &= K\ln(1+C)\,. \end{aligned} \tag{44}$$

The L^2 distance in Eq. (41) increases with intensity level I. On the other hand, for the cases $0 < a < 1$, the Weberized distances are, to leading order, constant as $I \to \infty$ and constant for all I in the case $a = 1$.

That the Weberized distance is constant only to leading order for the case $0 < a < 1$ may be explained by the fact that only the leading order term $1/y^a$ of the density function $\rho_a(y)$ was used in the definition of the Weberized measure $D_{2,a}$. It would be interesting to see if the inclusion of higher order terms of the asymptotic expansion for $\rho_a(y)$ would yield constancy to higher order in I.

5.1 Best approximations

In what follows, we let $\{\phi_k\}_{k=1}^\infty$ denote a set of real-valued functions that form a complete basis of $L^2(X)$. Now let $u \in \mathcal{F}(X) \subset L^2(X)$ denote the fixed reference signal/image function to be approximated. We are interested in best approximations to u having the following standard form,

$$v_n(x) = \sum_{k=1}^{n} c_k \phi_k(x)\,, \quad n = 1, 2, \ldots\,, \tag{45}$$

for $n \geq 1$.

For purposes of comparison, let us recall that in the classical case, i.e., when $u \in L^2(X)$, the (unique) **best approximation** of u in the subspace $V_n = \text{ span } \{\phi_1, \ldots, \phi_n\} \subset L^2(X)$ is given by

$$v_n = \arg \min_{v \in V_n} d_2(u, v)\,. \tag{46}$$

In the special case that the ϕ_k-basis is orthonormal we have, from the Projection Theorem, that the coefficients c_k are the **Fourier coefficients** of u, i.e.,

$$c_k = \langle u, \phi_k \rangle\,, \quad 1 \le k \le n\,. \tag{47}$$

In the present study, however, where the function u to be approximated is an element of the space $\mathcal{F}(X)$ defined earlier, we face the complication that the approximation functions $v_n(x)$ defined in Eq. (45) must also lie in $\mathcal{F}(X)$, i.e., $A \le u_n(x) \le B$ for a.e. $x \in X$. For each $n \ge 1$, we therefore define the following feasible parameter set, $C_n \subset \mathbb{R}^n$,

$$C_n = \left\{ \mathbf{c} = (c_1, \ldots, c_n) \in \mathbb{R}^n \;\middle|\; v_n(x) = \sum_{k=1}^{n} c_k \phi_k(x) \;\in\; \mathcal{F}(X) \right\}. \tag{48}$$

By definition, $C_n \subset C_{n+1}$ for $n \ge 1$. Clearly, the subsets C_n depend on the choice of basis set $\{\phi_k\}_{k=1}^{\infty}$. In what follows, we assume that the ϕ_k satisfy some rather generic conditions:

1. $\phi_1(x) = K > 0$, a constant, for all $x \in X$.
2. There exists a constant $M > 0$ such that $|\phi_k(x)| \le M$ for all $k \ge 2$. (In the case of an sine/cosine basis with no normalization constants, $M = 1$.)
3. For each $k \ge 2$, there exists at least one $\bar{x} \in X$ for which $\phi_k(\bar{x}) = 0$.

The following theorem is proved in Li (2020).

Theorem 9 *For all $n \ge 1$, the subsets $C_n \subset \mathbb{R}^n$ are compact and convex.*

We now use the subets $C_n \in \mathbb{R}^n$ to define the following subsets $S_n \subset \mathcal{F}(X)$ for $n \ge 1$,

$$S_n = \left\{ v : X \to \mathbb{R}_g \;\middle|\; v(x) = \sum_{k=1}^{n} c_k \phi_k(x) \quad \text{for} \quad \mathbf{c} \in C_n \right\}. \tag{49}$$

Definition 3 For each $n \ge 1$, let $\psi_n : C_n \to S_n$ be defined as follows. For a given $\mathbf{a} = (a_1, \ldots, a_n) \in C_n$, define

$$v_n(x) = \sum_{k=1}^{n} a_n \phi_n(x) \quad \text{for all} \quad x \in X\,. \tag{50}$$

By construction, $v_n \in S_n$. We denote v_n as $\psi_n(\mathbf{a})$.

Theorem 10 *For each $n \geq 1$, the mapping $\psi_n : C_n \to S_n$ is a homeomorphism.*

Proof Very briefly, the linear independence of the basis functions $\{\phi_1, \ldots, \phi_n\}$ implies that ψ_n is a bijection. From the equivalence of the D_a and d_2 metrics in S_n, we may use the d_2 metric to easily show that for $\mathbf{a}, \mathbf{b} \in C_n$,

$$d_2(\psi_n(\mathbf{a}, \psi_n(\mathbf{b}))) = [(\mathbf{a} - \mathbf{b})^T \mathbf{S}(\mathbf{a} - \mathbf{b})]^{1/2}\,, \tag{51}$$

where the elements of the symmetric (and nonsingular) overlap matrix $\mathbf{S}$ are $s_{ij} = \langle \phi_i, \phi_j \rangle$. Continuity of ψ_n and ψ_n^{-1} follows. □

Corollary *For each $n \geq 1$, the subset $S_n \subset \mathcal{F}(X)$ defined in* Eq. (49) *is compact and convex.*

The subsets S_n, $n \geq 1$, will play the role of approximation spaces in our best Weberized approximation problem. Let us recall that for any $n \geq 1$, the subset $S_n \subset \mathcal{F}(X)$ is **not** a linear space because of restrictions, stated earlier, that must be satisfied by a function $u \in \mathcal{F}(X)$. (The S_n are subsets of the approximation spaces $V_n =$ span $\{\phi_1, \ldots, \phi_n\}$ used in the classical best L^2 approximation problem.)

Our "best Weberized" approximation problem using intensity-based measures may now be defined as follows.

Definition 4 For a given Weber measure ν_a with density function ρ_a and a given $n \geq 1$, we define the **best approximation** $v_n \in S_n$ to $u \in \mathcal{F}(X)$ as follows,

$$v_n = \arg \min_{v \in S_n} D_{2,a}(u, v)\,, \tag{52}$$

where the metrics $D_{2,a}$ are defined in Eq. (40). The existence and uniqueness of such a best approximation will be proved below.

The existence of a solution v_n to Eq. (52) is guaranteed by the following result.

Theorem 11 *For a fixed $u \in \mathcal{F}(X)$ and $a > 0$, consider the functional $h : \mathcal{F}(X) \to \mathbb{R}$ defined as $h(v) = D_{2,a}(u, v)$ for $v \in \mathcal{F}(X)$. Then $h(v)$ is a continuous function of v.*

Proof From Eq. (40), $h(v) = \|P_a(u) - P_a(v)\|_2$, where $P_a(u) = u^{-a+1}$ for $0 \leq a < 1$ and $P_1(u) = \ln u$, and $\|\cdot\|_2$ denotes the L^2 norm on X—see Eq. (2). The continuity of $h(v)$ follows trivially from the continuity of both the L^2 norm and the function P_a. □

For each $n \geq 1$, it follows from the continuity of $h : \mathcal{F}(X) \to \mathbb{R}$ and the compactness of S_n that a solution to Eq. (52) exists. In order to establish uniqueness of the solution v_n to Eq. (52), we define the following sets of functions. For a fixed $a \in (0, 1]$ and an $n \geq 1$, let

$$T_n := \{P_a \circ u \mid u \in S_n\}\,. \tag{53}$$

Theorem 12 *Let $a \in (0, 1]$ be fixed. Then for all $n \geq 1$, the subsets $T_n \subset L^2(X)$ are convex.*

Proof In what follows, we consider a fixed value of the Weber exponent $a \in (0, 1]$. (The case $a = 0$ is trivial.) For any $n \geq 1$, suppose that $u, v \in S_n$, i.e.,

$$u(x) = \sum_{k=1}^{n} a_k \phi_k(x)\,, \quad v(x) = \sum_{k=1}^{n} b_k \phi_k(x)\,, \tag{54}$$

for $\mathbf{a}, \mathbf{b} \in C_n$. From the definition of the subset T_n, the functions $U = P_a(u)$ and $V = P_a(v)$ are elements of T_n. If T_n is convex then for any $\lambda \in [0, 1]$,

$$W_\lambda = \lambda U + \lambda V \in T_n\,. \tag{55}$$

We now show that for each $\lambda \in [0, 1]$, there exists a function $w_\lambda \in S_n$ such that $P_a(w_\lambda) = W_\lambda$, which implies that $W_\lambda \in T_n$. For the case $0 \leq a \leq 1$, this means that

$$[w_\lambda(x)]^b = \lambda[u(x)]^b + (1 - \lambda)[v(x)]^b\,, \quad \forall x \in X\,, \tag{56}$$

where $b = -a + 1$. For the case $a = 1$, this means that

$$\ln w_\lambda(x) = \lambda \ln u(x) + (1 - \lambda)v(x)\,, \quad \forall x \in X\,. \tag{57}$$

Here we consider the case $0 < a < 1$: The proof for the case $a = 1$ proceeds in a similar fashion. From Eq. (56) and the fact that $u, v \in S_n \subset \mathcal{F}(X)$, it is easy to show that $A \leq w_\lambda(x) \leq B$ for a.e. $x \in X$, which implies that $w_\lambda \in \mathcal{F}(X)$.

If, for any $n \geq 1$, $w_\lambda \in S_n$ it admits the following expansion,

$$w_\lambda(x) = \sum_{k=1}^{n} c_k(\lambda)\phi_k(x)\,. \tag{58}$$

Substitution of this expansion into Eq. (56) yields the following equation,

$$\left[\sum_{k=1}^{n} c_k(\lambda)\phi_k(x)\right]^b = \lambda\left[\sum_{k=1}^{n} a_k\phi_k(x)\right]^b + (1 - \lambda)\left[\sum_{k=1}^{n} b_k\phi_k(x)\right]^b\,, \quad \forall x \in X\,. \tag{59}$$

We now prove, using induction, that for each $n \geq 1$, a unique solution to Eq. (59) exists, i.e., a unique set of coefficients, $c_k(\lambda), 1 \leq k \leq n$. Note the following "boundary values" for the coefficients $c_k(\lambda)$:

$$c_k(0) = b_k\,, \quad c_k(1) = a_k\,, \quad 1 \leq k \leq n\,. \tag{60}$$

Case $n = 1$: In this case, the only basis function used in the expansion is $\phi_1(x) = K$. Substitution into (59) followed by division of both sides by K^b yields the result,

$$c_1(\lambda)^b = \lambda a_1^b + (1-\lambda)b_1^b \implies c_1(\lambda) = \left[\lambda a_1^b + (1-\lambda)b_1^b\right]^{1/b}. \tag{61}$$

This implies the existence of w_λ for $n = 1$ which, in turn, implies that T_1 is convex. (The uniqueness of such a w_λ follows from Theorem 10.)

Case $n = 2$: Equation (59) becomes

$$[c_1(\lambda)\phi_1(x) + c_2(\lambda)\phi_2(x)]^b = \lambda[a_1\phi_1(x) + a_2\phi_2(x)]^b + (1-\lambda)[b_1\phi_1(x) + b_2\phi_2(x)]^b. \tag{62}$$

Since this equation must be satisfied for all $x \in X$, let $x = \bar{x} \in X$ which is a zero of $\phi_2(x)$, i.e., $\phi_2(\bar{x}) = 0$. (Recall that the existence of at least one zero for the $\phi_k(x)$, $k \geq 1$, is assumed.) Setting $x = \bar{x}$ in (62) produces the same equation as obtained in the case $n = 1$. After division by K^b, Eq. (62) becomes Eq. (61), implying that we have the same solution for $c_1(\lambda)$ as in the case $n = 1$.

To find $c_2(\lambda)$ let $x = p \in X$ such that $\phi_2(p) = P$ for any nonzero $P \in$ Range (ϕ_2). Setting $x = p$ in Eq. (62) yields

$$[c_1(\lambda)K + c_2(\lambda)P]^b = \lambda[a_1K + a_2P]^b + (1-\lambda)[b_1K + b_2P]^b. \tag{63}$$

Since $c_1(\lambda)$ is known, we may solve for $c_2(\lambda)$. This proves the existence of w_λ for $n = 2$. Hence T_2 is convex. (Once again, the uniqueness of w_λ follows from Theorem 10.)

We now assume that a solution to Equation (59) exists for $n = N > 1$ and prove that a solution exists for $n = N + 1$. For $n = N + 1$, Eq. (59) becomes

$$\begin{aligned}\lambda[c_1(\lambda)\phi_1(x) + \cdots + c_N(\lambda)\phi_n(x) + c_{N+1}\phi_{n+1}(x)]^b \\ = \lambda[a_1\phi_1(x) + \cdots + a_N\phi_n(x) + a_{N+1}\phi_{n+1}(x)]^b \\ + (1-\lambda)[b_1\phi_1(x) + \cdots + b_N\phi_n(x) + b_{N+1}\phi_{n+1}(x)]^b.\end{aligned} \tag{64}$$

If we set $x = \bar{x} \in X$, where $\phi_{n+1}(\bar{x}) = 0$, then the above equation becomes Eq. (59) in the case $n = N$ and $x = \bar{x}$ for which a solution is assumed to exist. Therefore, we know $c_k(\lambda)$ for $1 \leq k \leq N$. Now set $x = p \in X$ such that $\phi_{N+1}(p) = P \neq 0$ where $P \in$ Range (ϕ_{N+1}) in Eq. (64). The result is an equation which allows $c_{N+1}(\lambda)$ to be expressed in terms of the known coefficients $c_k(\lambda)$, $1 \leq k \leq N$. This proves the existence of w_λ for $n = N + 1$. Hence T_{N+1} is convex. By induction, for the case $0 < a < 1$, T_n is convex for all $n \geq 1$.

The same inductive proof may be used for the case $a = 1$ involving the logarithm function—see Eq. (57). □

Comments

1. For each $n \geq 1$, the coefficients $c_k(\lambda), 1 \leq k \leq n$, perform a **nonlinear interpolation** between the coefficients a_k and b_k. This is seen in Eq. (61) for the special case $c_1(\lambda)$.
2. It is interesting that the coefficients $c_k(\lambda), 1 \leq k \leq N$, of $w_\lambda \in S_N$ are used in the expansion for $w_\lambda \in S_{N+1}$ even though the ϕ_k basis is not necessarily orthonormal.

We simply "build up" the functions $w_\lambda \in S_n$ in the same way as is done in Hilbert space using an orthonormal basis and the Projection Theorem.

We now establish the uniqueness of the solution v_n to Eq. (52) using the facts that (i) $T_n \subset L^2(X)$ and (ii) $L^2(X)$ is a **strictly normed space** Lebedev et al. (2003), i.e., if

$$\|x+y\|_2 = \|x\|_2 + \|y\|_2\,, \quad x \neq 0\,, \tag{65}$$

then $y = \lambda x$ and $\lambda \geq 0$, where $\|\cdot\|_2$ denotes the L^2 norm.

Theorem 13 *Let $u \in \mathcal{F}(X)$. Then for a given $n \geq 1$ and $a \in (0,1]$, the solution to* Eq. (52) *is unique.*

Proof If $u \in S_n$, then there is only one minimizer, $v_n = u$. Now suppose that $u \notin S_n$ and that there are two minimizers of $D_{2,a}(u,v)$, namely, $v_{n,1}, v_{n,2} \in S_n$ with $v_{n,1} \neq v_{n,2}$. Thus,

$$\Delta_{2,a}(u, v_{n,1}) = \Delta_{2,a}(u, v_{n,2}) = \min_{v \in S_n} \Delta_{2,a}(u,v) = d > 0\,. \tag{66}$$

Recalling the definition of $h(v)$ in Theorem 11, we have that

$$h(v_{n,1}) = h(v_{n,2}) = d\,, \tag{67}$$

which may be expressed in terms of the L^2 norm as follows,

$$\|P_a(u) - P_a(v_{n,1})\|_2 = \|P_a(u) - P_a(v_{n,2})\|_2 = d > 0\,, \tag{68}$$

where $P_a(u) = u^{-a+1}$ for $0 < a < 1$ and $P_1(u) = \ln u$. Since $v_{n,1}, v_{n,2} \in S_n$, it follows from Eq. (53) that $P_a(v_{n,1}), P_a(v_{n,2}) \in T_n$. Since T_n is convex (Theorem 12), the following function,

$$W_n = \frac{1}{2}(P_a(v_{n,1}) + P_a(v_{n,2}))\,, \tag{69}$$

lies in T_n. From Theorem 10, there exists a unique $w_n \in S_n$ such that $P_a(w_n) = W_n$. Furthermore,

$$\Delta_{2,a}(u, w_n) = h(w_n) = \|P_a(u) - P_a(w_n)\|_2 \geq d\,. \tag{70}$$

But

$$\begin{aligned} \|P_a(u) - P_a(w_n)\|_2 &= \left\| P_a(u) - \frac{1}{2}(P_a(v_{n,1}) + P_a(v_{n,2})) \right\|_2 \\ &\leq \left\| \frac{1}{2}(P_a(u) - P_a(v_{n,1})) \right\|_2 + \left\| \frac{1}{2}(P_a(u) - P_a(v_{n,2})) \right\|_2 \\ &\leq \frac{1}{2}\|P_a(u) - P_a(v_{n,1})\|_2 + \frac{1}{2}\|P_a(u) - P_a(v_{n,2})\|_2 \\ &= d\,. \end{aligned} \tag{71}$$

From (70) and (71) it follows that $\|P_a(u) - P_a(w_n)\|_2 = d$ which may be expressed as follows,

$$\left\|P_a(u) - \frac{1}{2}(P_a(v_{n,1}) + P_a(v_{n,2}))\right\|_2 = \left\|\frac{1}{2}(P_a(u) - P_a(v_{n,1}))\right\|_2 + \left\|\frac{1}{2}(P_a(u) - P_a(v_{n,2}))\right\|_2 . \tag{72}$$

Now using the fact that $L^2(X)$ is a strictly normed space and making the following identifications in Eq. (65),

$$x = \frac{1}{2}(P_a(u) - P_a(v_{n,1}))\,, \quad y = \frac{1}{2}(P_a(u) - P_a(v_{n,2}))\,, \tag{73}$$

it follows that $y = \lambda x$ for some $\lambda \geq 0$, i.e.,

$$P_a(u) - P_a(v_{n,1}) = \lambda(P_a(u) - P_a(v_{n,2}))\,. \tag{74}$$

Taking norms, we have

$$\|P_a(u) - P_a(v_{n,1})\|_2 = \lambda\|P_a(u) - P_a(v_{n,2})\|_2\,. \tag{75}$$

From Eq. (68), $\lambda = 1$ which, from Eq. (74), implies that $P_a(v_{n,1}) = P_a(v_{n,2})$. From Theorem 10, this implies that $v_{n,1} = v_{n,2}$ which contradicts the original assumption that the two minimizers are unequal. Therefore there can be at most one minimizer of $\Delta_{2,a}(u, v)$ in S_n. □

For the practical problem of finding best approximations in the cases $a \in [0, 1]$, it is more convenient to work with the squared distance function, expressed as a function of the expansion coefficients c_k of v_n,

$$\begin{aligned}[D_{2,a}(u, v_n)]^2 &= \int_X [P_a(u(x)) - P_a(v_n(x))]^2\, dx \\ &= \int_X \left[P_a(u(x)) - P_a\left(\sum_{k=1}^{n} c_k\phi_k(x)\right)\right]^2 dx \\ &=: g(\mathbf{c})\,,\end{aligned} \tag{76}$$

where $P_a'(y) = \rho_a(y) = 1/y^a$ and $\mathbf{c} = (c_1, \ldots, c_n)$. The optimization problem in Eq. (52) then becomes the following problem,

$$\mathbf{a} = (a_1, \ldots, a_n) = \arg\min_{\mathbf{c}\in C_n} g(\mathbf{c})\,, \tag{77}$$

the solution of which yields the best approximation $u_n \in S_n$,

$$u_n(x) = \sum_{k=1}^{n} a_k\phi_k(x)\,. \tag{78}$$

From Theorems 10 and 13, this solution exists and is unique.

Example 1 We consider the following step function on $X = [0, 1]$.

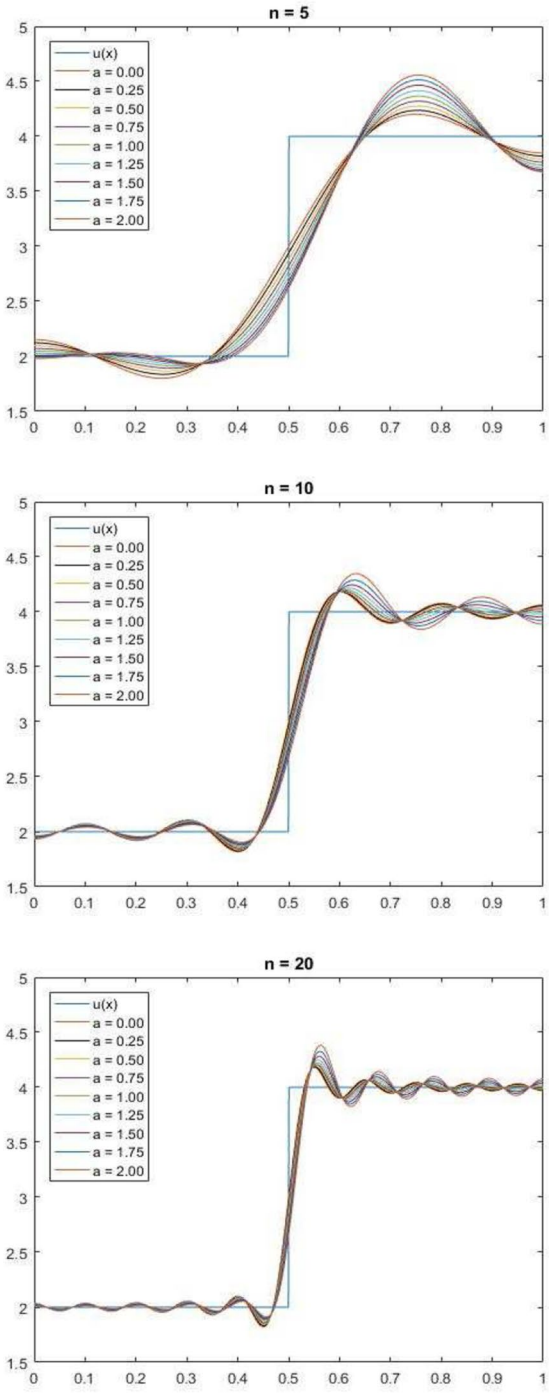

Fig. 3 Best Weberized approximations v_n to the step function $u(x)$ in Eq. (79) for $a = 0.25, 0.50, \ldots, 2.0$ along with best L^2 approximation ($a = 0$) for comparison. The function $u(x)$ was sampled at $N = 1024$ equidistant points on [0, 1] and an $N = 1024$-point DCT basis function set was used. Top: $n = 5$ basis functions used. Middle: $n = 10$. Bottom: $n = 20$

$$u(x) = \begin{cases} 2, & 0 \le x \le \frac{1}{2}, \\ 4, & \frac{1}{2} < x \le 1. \end{cases} \tag{79}$$

In Fig. 3 are shown plots of the function $u(x)$ along with best approximations $v_n(x)$ for the cases $a = 0$ (best L^2), $a = 0.25, 0.5, \ldots, 2.0$, using $n = 5$ (top), $n = 10$ (middle) and $n = 20$ (bottom) basis functions. The basis functions ϕ_k used here were the 1D discrete cosine transform (DCT) basis functions used in the JPEG compression method. The function $u(x)$ was sampled at $N = 1024$ equidistant points, $x_i = i/N$, $i = 0, 1, 2, \ldots, N$. The approximations $v_n(x)$ were then found by minimizing the appropriate squared D_2-distance function $[\Delta_{2,a}(u, v_n)]^2$ in Eq. (76) using a simple gradient-descent method.

The best Weberized approximations $v_n(x)$ for $a > 0$ are seen to provide better approximations of $u(x)$ than the $a = 0$ (best L^2) approximation over the interval [0, 0.5] and poorer approximations over the interval [0.5, 1], as expected. Moreover, the degree of "goodness" over [0, 0.5] and "poorness" over [0.5, 1] of the best Weberized approximations increases with the Weber exponent a, also as expected since the density function $\rho(y) = 1/y^a$ decreases more rapidly with increasing a.

Technically speaking, only the results $0 < a \le 1$ presented in Fig. 3 correspond to the generalized Weber measures $\rho_a(y) = 1/y^a$ of Eq. (39) studied theoretically in this section. That being said, the results obtained by using $D_{2,a}$ distances for $a > 1$—computed from the first formula in Eq. (40)—are also valid since Theorem 5 applies to these integrands as well. (The functions $P_a(y) = y^{-a+1}$ are strictly decreasing over $[A, B]$ and therefore invertible.) These results are noteworthy since the pattern of "Weberization" continues with increasing a. Moreover, the entire set of results presented in the figure for $0 < a \le 2$ very closely resembles those obtained from the intensity-dependent weight function approach and presented in Urbaniak et al. (2020).

6 Concluding remarks

In this paper, we have provided further mathematical analysis of a method, introduced in Li et al. (2018, 2019), which Weberizes the L^2 metric by employing measures supported on the (positive) range space $\mathbb{R}_g = [A, B]$ of the functions concerned. In particular, we have analyzed the best Weberized approximation associated with these metrics in more detail by defining appropriate spaces—$C_n \in \mathbb{R}_n$, $S_n \in \mathcal{F}(X)$ and $T_n \in L^2(X)$—over which the optimization problem is defined. A proof of the existence and uniqueness of the best approximation v_n for a given values of $a \in (0, 1]$ and n, the number of basis functions employed, has been provided.

We claim that the "equal area condition" of Eq. (14) represents a unique way of looking at Weber's generalized model of perception. Not only is it interesting from a theoretical, i.e., mathematical, perspective but it also yields a concrete result, namely, a measure ν_a defined by a density function $\rho_a(y)$ which, in turn, defines a metric which "conforms" to Weber's model. It would be most interesting to investigate whether such a condition, or suitable modification thereof, applies to other

models, not only in signal and image processing, but in applied mathematics in general.

Finally, we mention that our Weberized approach can, at least in principle, be used in any standard image processing problem, e.g., image denoising. For example, in the case of total variation (TV) denoising, one approach would be simply to replace the L^2 distance normally used in the fidelity term with a Weberized distance, i.e., given a noisy image $\tilde{u} \in \mathcal{F}(X)$, find

$$u = \arg \min_{v \in \mathcal{F}(X)} D_{2,a}(\tilde{u}, v) + \lambda \|v\|_{TV}\,, \tag{80}$$

for an appropriate value of the Weber exponent, $a > 0$, where the Weberized metrics $D_{2,a}$ are defined in Eq. (40) and where $\|\cdot\|_{TV}$ denotes a total variation norm. We are currently investigating such approaches.

Acknowledgements We gratefully acknowledge that this research has been supported in part by the Natural Sciences and Engineering Research Council of Canada (NSERC) in the form of a Discovery Grant (ERV). Financial support from the Department of Applied Mathematics and the Faculty of Mathematics, University of Waterloo in the form of Teaching Assistantships (DL) are also acknowledged with much appreciation and thanks.

References

Belitskii G, Lyubich Y (1988) The Abel equation and total solvability of linear functional equations. Stud Math 127(1):81–97

Cornsweet TN, Pinsker HM (1965) Luminance discrimination of brief flashes under various conditions of adaptation. J Physiol 176:294310

Forte B, Vrscay ER (1995) Solving the inverse problem for function and image approximation using iterated function systems. Dyn Contin Discrete Impul Syst 1:177–231

Girod B (1993) What's wrong with mean squared error? In: Watson AB (ed) Digital images and human vision. MIT Press, Cambridge

Halpern Andrea R, Darwin Christopher J (1982) Duration discrimination in a series of rhythmic events. Percept Psychphys 31:8689

Kingdom F, Whittle P (1996) Contrast discrimination at high contrasts reveals the influence of local light adaptation on contrast processing. Vis Res 36(6):817–829

Kowalik-Urbaniak IA (2014) The quest for "diagnostically lossless" medical image compression using objective image quality measures. Ph.D. Thesis, Department of Applied Mathematics, University of Waterloo

Kowalik-Urbaniak IA, La Torre D, Vrscay ER, Wang Z (2014) Some Weberized L^2-based methods of signal/image approximation. Image Analysis and Recognition, ICIAR 2014. LNCS 8814:20–29

Lebedev LP, Vorovich II, Gladwell GML (2003) Functional analysis, applications in mechanics and inverse problems, 2nd edn. Kluwer, New York

Li D (2020) A novel class of intensity-based metrics for image functions which accommodate a generalized Weber's model of perception. Thesis, Department of Applied Mathematics, University of Waterloo, M.Math

Li Z, Kou X, Cao H, Man X (2014) The HIS_MSR algorithm for foggy image enhancement. Appl Mech Mater 577:806–809

Li D, La Torre D, Vrscay ER (2018) The use of intensity-based measures to produce image function metrics which accommodate Weber's models of perception. Image Analysis and Recognition, ICIAR 2018. LNCS 10882:326–335

Li D, La Torre D, Vrscay ER (2019) Existence, uniqueness and asymptotic behaviour of intensity-based measures which conform to a generalized Weber's model of perception. Image Analysis and Recognition, ICIAR 2019. LNCS 11662:297–308
Michon JA (1966) Note on the generalized form of Weber's Law. Percept Psychophys 1:329–330
Oppenhein AV, Schafer RW, Stockhan TG Jr (1968) Nonlinear filtering of multiplied and convolved signals. Proc IEEE 56(8):1264–1291
Pinoli J-C (1997) The logarithmic image processing model: connections with human brightness perception and contrast estimators. J Math Imaging Vis 7:341–358
Shen J (2003) On the foundations of vision modeling I. Weber's law and Weberized TV restoration. Phys D 175:241–251
Shen J, Jung YM (2006) Weberized Mumford-Shah model with Bose-Einstein photon noise. Appl Math Optim 53:331–358
Small C (2007) Functional equations and how to solve them. Springer, New York
Targonski G (1981) Topics in iteration theory. Vandenhoeck & Ruprecht, Göttingen
Urbaniak IA, Kunze AG, Li D, Vrscay ER (2020) The use of intensity-dependent weight functions to "Weberize" L^2-based methods of signal and image approximation, preprint
Wandell BA (1995) Foundations of vision. Sinauer Publishers, Sunderland
Wang Z, Bovik AC (2009) Mean squared error: Love it or leave it? A new look at signal fidelity measures. IEEE Sig Proc Mag 26:98–117
Wang Z, Bovik AC, Sheikh HR, Simoncelli EP (2004) Image quality assessment: from error visibility to structural similarity. IEEE Trans Image Proc 13(4):600–612
Wang Z, Li Q (2011) Information content weighting for perceptual image quality assessment. IEEE Trans Image Proc 20(5):1185–1198